BU
ARPA-E-72

Division of Engineering
BROWN UNIVERSITY
PROVIDENCE, R. I.

GUIDED SURFACE WAVES ON AN ISOTROPIC ELASTIC HALF-SPACE

L. B. FREUND

TECHNICAL LIBRARY
ABERDEEN PROVING GROUND, MD
STEAP-TL

AD707079

Department of Defense
Advanced Research Projects Agency
Contract SD-86
Materials Research Program

ARPA E72

May 1970

BU
ARPA-E-72

Guided Surface Waves on an Isotropic Elastic Half-Space[1]

L. B. Freund

Assistant Professor of Engineering
Brown University
Providence, Rhode Island 02912

1. Water propagation

TECHNICAL LIBRARY

ABERDEEN PROVING GROUND, MD
STEAP-TL

[1]The research support of the Advanced Research Projects Agency, Department of Defense, is gratefully acknowledged.

20060223352

[redacted]

Abstract

Three-dimensional wave propagation in an elastic half-space is considered. The half-space is traction free on half its boundary, while the remaining part of the boundary is free of shear traction and is constrained against normal displacement by a smooth, rigid barrier. A time-harmonic surface wave, traveling on the traction free part of the surface, is obliquely incident on the edge of the barrier. The amplitude and the phase of the resulting reflected surface wave are determined by means of Laplace transform methods and the Wiener-Hopf technique. Wave propagation in an elastic half-space in contact with two rigid, smooth barriers is then considered. The barriers are arranged so that a strip on the surface of uniform width is traction free, which forms a wave-guide for surface waves. Results of the surface wave reflection problem are then used to geometrically construct dispersion relations for the propagation of unattenuated guided surface waves in the guiding structure. The rate of decay of body wave disturbances, localized near the edges of the guide, is discussed.

Introduction

It has recently been discovered that surface waves, propagating on a plane surface of an elastic solid, can be guided over significant distances by introducing barriers on the surface of the substrate in various ways. The substrate is usually viewed as an elastic half-space, and the barriers are formed by depositing a layer of another elastic material on part of the surface of the half-space. By depositing a relatively massive, elastically weak material along a strip on the surface, or by depositing a relatively light, elastically stiff material on all parts of the surface except along a strip, a structure which will act as a waveguide for elastic surface waves is obtained. A detailed discussion of some guiding structures has been given by Tiersten [1], who was concerned primarily with obtaining approximate dispersion relations for harmonic waves propagating in the waveguides. The guided waves in these cases are not the usual types of surface waves with constant amplitude on lines of constant phase, but are more general surface waves, of the type discussed by Knowles [2], that have amplitudes which vary along lines of constant phase.

In [1], Tiersten modeled the surface displacements of the guiding structure by the transverse deflections of an appropriately selected system of membranes to obtain approximate dispersion relations for the waveguide. A somewhat different approach is proposed here. Before dispersion relations are studies, an auxiliary problem is considered in which one edge of the guiding structure is moved off to infinity, so that only one discontinuity in the boundary conditions must be taken into account. The reflection and transmission of surface

TECHNICAL LIBRARY
ABERDEEN PROVING GROUND, MD
STEAP-TL

waves at the discontinuity is then studied by solving the appropriate equations of dynamic elasticity. The elasticity problem is three-dimensional, in the sense that the scalar dilatational displacement potential and more than one component of the vector shear wave potential are nonzero. The problem can be transformed, however, so that all unknown quantities are solutions of two-dimensional boundary value problems which can be solved by Laplace transform methods and the Wiener-Hopf technique [3].

The solution of the surface wave reflection problem is then used to find approximate dispersion relations for the waveguide. The solution of the reflection problem indicates the presence of localized body wave disturbances near the edge of the barrier. The approximate dispersion relations for free waves in the guide are obtained by geometrical considerations, assuming that these localized disturbances decay sufficiently fast with distance from either edge of the guide.

The particular problem considered in detail in the following sections was chosen for its simplicity, and it serves as a convenient vehicle for presenting the method. The boundary conditions considered assume that the surface of the isotropic elastic half space is traction free on a strip of finite width and that the remaining part of the surface is free of shear traction and undergoes no displacement in the direction normal to the surface. Systems which are more realistic, in that the mass and stiffness of the loading are considered, are currently being studied.

Concerning applications, there is a considerable effort being exerted by workers in electronics to design and fabricate structures to act as surface wave guides at microwave frequencies. Configurations other

than those mentioned above are being studied. These devices are being integrated into miniature circuits and serve as transmission lines, delay lines, amplifiers, mixers, etc. A review of the state of development of these devices is given by Stern [4].

The Surface Wave Reflection Problem

Let $x_j = (x, y, z)$ be a three-dimensional Cartesian coordinate system, oriented as in Fig. 1. The isotropic elastic solid occupies the region $z \geq 0$. The traction on the surface $z = 0$ vanishes for $x < 0$. For $x > 0$, the shear traction vanishes on $z = 0$, while the surface is constrained against displacement in the z-direction by a smooth, rigid obstacle. The edge of this impedance coincides with the y-axis.

The displacement vector is expressed in terms of a dilatational wave potential Φ and a vector shear wave potential Ψ_k as[2]

$$U_j = (U, V, W) = \Phi_{,j} + e_{jk\ell}\,\Psi_{k,\ell} \quad . \tag{1}$$

The potential functions satisfy the wave equations

$$\nabla^2\Phi - a^2\ddot{\Phi} = 0 \quad , \quad \nabla^2\Psi_j - b^2\ddot{\Psi}_j = 0 \quad , \quad j = 1, 2, 3 \quad , \tag{2}$$

where a and b are the dilatational and shear wave slownesses, and the dot denotes differentiation with respect to time. The divergence of Ψ_j is arbitrary and, for definiteness, is taken to be zero,

$$\Psi_{j,j} = 0 \quad . \tag{3}$$

The components of the stress tensor are given in terms of the displacement

[2]Cartesian tensor notation is used whenever it is convenient to do so.

potentials as

$$\Sigma_{jk} = \lambda'\delta_{jk}\Phi_{,\ell\ell} + 2\mu\Phi_{,jk} + \mu(e_{k\ell m}\Psi_{m,\ell j} + e_{j\ell m}\Psi_{m,\ell k}) \tag{4}$$

where λ' and μ are the Lamé constants.

The displacement potentials which solve the problem posed must satisfy the following conditions on the boundary $z = 0$ for $-\infty < y < \infty$:

$$\Sigma_{zz} = 0 \quad , \quad -\infty < x < 0 \tag{5}$$

$$\Sigma_{xz} = 0 \quad , \quad \Sigma_{yz} = 0 \quad , \quad -\infty < x < \infty \tag{6}$$

$$W = 0 \quad , \quad 0 < x < \infty \quad . \tag{7}$$

The input is a free surface Rayleigh wave with harmonic time dependence which is propagating in the region $x < 0$, and which is obliquely incident on the obstacle covering the region $x > 0$. A line of constant phase is shown in Fig. 1(b), where the angle of incidence θ_o is defined. If the Rayleigh wave slowness for the material at hand is c and the circular frequency of the wave train is ω , then the incident wave is represented by

$$\Phi^o(x, y, z, t) = \phi^o e^{i(\omega t - \alpha x - \beta y)} e^{-p_o z} \tag{8a}$$

$$\Psi_j^o(x, y, z, t) = \psi_j^o e^{i(\omega t - \alpha x - \beta y)} e^{-q_o z} \tag{8b}$$

where ϕ^o is a constant amplitude, and α and β are components of the wave number $\gamma = \omega c$ in the x and y directions, that is, $\alpha = \gamma \sin\theta_o$ and $\beta = \gamma\cos\theta_o$. Furthermore,

$$p_o = (\gamma^2 - \kappa_a^2)^{1/2} \quad , \quad q_o = (\gamma^2 - \kappa_b^2)^{1/2} \quad , \tag{9a}$$

$$\psi_1^o = \frac{i\beta(2\gamma^2 - \kappa_b^2 - 4p_o q_o)}{2q_o(\gamma^2 - \kappa_b^2)} \phi^o \quad , \tag{9b}$$

$$\psi_2^o = -\frac{\alpha}{\beta}\psi_1^o \quad , \quad \psi_3^o = 0 \quad , \tag{9c}$$

where $\kappa_a = \omega a$ and $\kappa_b = \omega b$. It is the response of the material to this surface wave input that is sought.

It is now assumed that the surface wave represented by (8) is present for all x , and the potentials are written in the form

$$\Phi(x, y, z, t) = \phi(x, z)\, e^{i(\omega t - \beta y)} + \Phi^o(x, y, z, t) \quad , \tag{10a}$$

$$\Psi_j(x, y, z, t) = \psi_j(x, z)\, e^{i(\omega t - \beta y)} + \Psi_j^o(x, y, z, t) \quad . \tag{10b}$$

It is the fact that the physical system is invariant with respect to translation in the y-direction that makes it possible to write the dependence of the potentials on y in the explicit form indicated in (10). All dependent variables are assumed to be split into a sum of two terms as in (10), one representing the incident surface wave and the second term representing the diffracted field. The convention adopted in writing (10) that a lower case symbol represents the amplitude of the diffracted field in the x, z-plane of the corresponding upper case symbol is taken to apply to all displacement components and stress components.

The potentials (10) are substituted into the wave equations (2), the condition (3) and the boundary conditions (5) - (7) to obtain a formulation of the boundary value problem for ϕ and ψ_j . The input surface wave appears in the formulation as the right side of a nonhomogeneous boundary condition. Omitting a common exponential factor,

the result of the substitution is

$$\nabla^2\phi - \lambda_a^2\phi = 0 \quad , \quad \nabla^2\psi_j - \lambda_b^2\psi_j = 0 \tag{11}$$

$$\psi_{1,1} - i\beta\psi_2 + \psi_{3,3} = 0 \quad , \tag{12}$$

$$\sigma_{zz}(x, 0) = 0 \quad , \quad -\infty < x < 0 \tag{13}$$

$$\sigma_{xz}(x, 0) = 0 \quad , \quad \sigma_{yz}(x, 0) = 0 \quad , \quad -\infty < x < \infty \tag{14}$$

$$w(x, 0) = - C_o e^{-i\alpha x} \quad , \quad 0 < x < \infty \tag{15}$$

where $\lambda_a^2 = \beta^2 - \kappa_a^2$, $\lambda_b^2 = \beta^2 - \kappa_b^2$ and C_o may easily be determined from (1) and (8).

The problem defined by (11) - (15) is solved by means of the bilateral Laplace transform and the Wiener-Hopf technique. The transform is defined by

$$\hat{\phi}(\lambda, z) = \int_{-\infty}^{\infty} e^{-\lambda x} \phi(x, z)dx \quad . \tag{16}$$

This transform is applied to the equations (11) - (15). The anticipated form of the solution suggests that all quantities are dominated by a term like $e^{-i\alpha|x|}$ as $|x|$ becomes large, which implies that all transforms converge only on the imaginary axis in the λ-plane. To apply the Wiener-Hopf method, however, a strip of convergence is required. The usual artifice employed to achieve this strip of convergence is to prescribe a slight material dissipation in such a way as to give α a small negative imaginary part. The Wiener-Hopf method is then applied, after which the dissipation is assumed to vanish. This scheme is well established [5], and no direct reference to it will be made in the subsequent development. One result of the scheme worth mentioning here is

that, for the present problem, the positive imaginary axis is viewed as being in the right half-plane while the negative imaginary axis is in the left half-plane. In other words, the inversion path for the transform (16) is the imaginary axis, approached from the right in the lower half of the λ-plane and approached from the left in the upper half-plane.

Application of the Laplace transform to (11) yields four ordinary differential equations whose solutions, bounded and/or representing outgoing waves for large z, are

$$\hat{\phi} = P(\lambda)e^{-pz} \quad , \quad p = (\lambda_a^2 - \lambda^2)^{1/2} \quad , \quad \mathrm{Re}(p) \geq 0 \tag{17a}$$

$$\hat{\psi}_j = Q_j(\lambda)e^{-qz} \quad , \quad q = (\lambda_b^2 - \lambda^2)^{1/2} \quad , \quad \mathrm{Re}(q) \geq 0 \tag{17b}$$

Assuming λ_a to be real, the condition $\mathrm{Re}(p) \geq 0$ is satisfied everywhere in the λ-plane if branch cuts are provided along $\lambda_a \leq |\mathrm{Re}(\lambda)| < \infty$, $\mathrm{Im}(\lambda) = 0$ and the branch whose value is λ_a at $\lambda = 0$ is chosen. As β becomes smaller, the branch point λ_a approaches the origin. The branch point reaches the origin when $\beta = \kappa_a$, and then moves up the imaginary axis, that is, λ_a becomes positive imaginary when $\beta < \kappa_a$. The branch cut then runs from λ_a to the origin along the imaginary axis, and then to $+\infty$ along the real axis. The situation is similar in the left half-plane. The particular case when λ_a is real and λ_b is imaginary is shown in Fig. 2.

The transform of (12) is

$$\lambda\hat{\psi}_1 - i\beta\hat{\psi}_2 + \hat{\psi}_{3,3} = 0 \quad . \tag{18}$$

Finally, the transformed boundary conditions are

$$\hat{\sigma}_{zz}(\lambda, 0) = \mu F_+(\lambda) \quad , \tag{19}$$

$$\hat{\sigma}_{xz}(\lambda, 0) = 0 \quad , \quad \hat{\sigma}_{yz}(\lambda, 0) = 0 \tag{20}$$

$$\hat{w}(\lambda, 0) = -\frac{C_o}{(\lambda + i\alpha)} + G_-^*(\lambda) \equiv \frac{G_-(\lambda)}{(\lambda + i\alpha)} \quad , \tag{21}$$

where $F_+(\lambda)$ is an unknown function, analytic in the right half of the λ-plane, and such that its inverse transform vanishes for $x < 0$. Similarly, the unknown function $G_-^*(\lambda)$ is analytic in the left half plane and is such that its inverse transform vanishes for $x > 0$. The boundary conditions are now applied to determine the parameters of integration P and Q_j.

A nonhomogeneous system of four linear algebraic equations for the four functions P and Q_j is obtained by substituting (17) into (18) - (20), and evaluating at $z = 0$. If the unknowns are ordered to form the vector (P, Q_1, Q_2, Q_3) and the equations are put in the order (19), $(20)_1$, $(20)_2$, (18), then the determinant of the coefficients is $\kappa_b^2 \, q \, D(\lambda)$, where

$$D(\lambda) \equiv (\lambda_b^2 + \beta^2 - 2\lambda^2)^2 + 4(\lambda^2 - \beta^2)pq \quad . \tag{22}$$

The function $D(\lambda)$ is a modified form of the Rayleigh wave function and, on the sheet of the Riemann surface being considered, $D = 0$ has only two roots in the finite λ-plane. These roots are located at $\lambda = \pm i\alpha$. The roots are indicated in Fig. 2. The solution of the system of equations is

$$P(\lambda) = (\lambda_b^2 + \beta^2 - 2\lambda^2) \, F_+(\lambda) \, / \, D(\lambda) \quad , \tag{23a}$$

$$Q_1(\lambda) = -2i\beta p \, F_+(\lambda) \, / \, D(\lambda) \quad , \tag{23b}$$

$$Q_2(\lambda) = -2\lambda p \, F_+(\lambda) \, / \, D(\lambda) \quad , \tag{23c}$$

$$Q_3(\lambda) = 0 \quad . \tag{23d}$$

The result (23) is now substituted into (21), yielding an equation of the Wiener-Hopf type

$$\kappa_b^2\, p(\lambda + i\alpha)\, F_+(\lambda) \;=\; D(\lambda)\, G_-(\lambda) \quad . \tag{24}$$

Strictly speaking, (24) holds only on the intersection line of the left and right half-planes. The function p is factored into the product p_+p_- where

$$p_{\pm} \;=\; (\lambda_a \pm \lambda)^{1/2} \quad . \tag{25}$$

To proceed with the Wiener-Hopf method, it is found to be convenient to introduce the auxiliary function $D^*(\lambda)$ defined by

$$D^*(\lambda) \;\equiv\; D(\lambda) \,/\, \kappa\, (\lambda^2 + \alpha^2) \quad , \tag{26}$$

where $\kappa = 2(\kappa_b^2 - \kappa_a^2) > 0$. This function has neither zeros nor poles in the cut λ-plane, and $D^*(\lambda) \to 1$ as $|\lambda| \to \infty$. A product factorization of D^* into sectionally analytic functions $D_+^*(\lambda)$ and $D_-^*(\lambda)$ (the plus and minus have the same meaning as before) has been presented in various forms many times in the literature, for example in [6] and [7]. It is merely noted here that such a factorization can be accomplished, and presentation of explicit expressions is deferred to a later point in the discussion.

The relation (24) can now be written

$$\frac{\kappa_b^2\, p_+\, F_+(\lambda)}{\kappa\, D_+^*(\lambda)} \;=\; \frac{(\lambda - i\alpha)\, D_-^*(\lambda)\, G_-(\lambda)}{p_-} \quad . \tag{27}$$

Applying the well-known analytic continuation argument, each side of (27) represents one and the same entire function, say $E(\lambda)$. From the

condition that $w(x, 0)$ is a continuous function of x at $x = 0$, coupled with the asymptotic result [8]

$$\lim_{x \to 0^-} w(x, 0) = \lim_{|\lambda| \to \infty} \lambda \hat{w}(\lambda, 0) ,$$

it is consluded that

$$G_-(\lambda) = o(1) \text{ as } |\lambda| \to \infty . \tag{28a}$$

It can also be shown that the condition of integrable strain energy density at $x = z = 0$ implies

$$F_+(\lambda) = o(1) \text{ as } |\lambda| \to \infty . \tag{28b}$$

In view of (28), $E(\lambda)$ has algebraic behavior at infinity and $E(\lambda) = o(\lambda^{1/2})$ as $|\lambda| \to \infty$. The extended Liouville theorem then implies that $E(\lambda) = E_o$, a constant, whose value can be determined by setting $\lambda = -i\alpha$ in the right side of (27). The functions $F_+(\lambda)$ and $G_-(\lambda)$ (or $G_-^*(\lambda)$) are then completely determined, and the transforms may be inverted.

Attention will be limited to the surface displacement on $z = 0$ and, in particular, on the z component of the surface displacement. The transform inversion integral for $w(x, 0)$ is

$$w(x, 0) = \frac{1}{2\pi i} \int_{-i\infty}^{i\infty} \frac{E_o\, p_-(\lambda)}{D_-^*(\lambda)\,(\lambda + i\alpha)(\lambda - i\alpha)} e^{\lambda x}\, d\lambda . \tag{29}$$

The path of integration is indicated in Fig. 2. For $x > 0$ the path of integration may be closed by an arc at infinity in the left half-plane. The only singularity of the integrand inside the resulting closed path is the pole at $\lambda = -i\alpha$, and the residue is found to exactly cancel the contribution of the incident wave for $x > 0$, thus satisfying the

boundary condition (7).

In the right half-plane the integrand of (29) has branch points at $\lambda = \lambda_a, \lambda_b$ and a pole at $\lambda = i\alpha$. For $x < 0$ the path of integration may be closed by an arc at infinity in the right half-plane. By applying Cauchy's theorem, $w(x, 0)$ may be written as a sum of the residue of the pole and a branch line integral, the latter representing the contribution due to body waves. The residue, on the other hand, represents the reflected surface wave which is the wave of primary interest here. Denoting the residue by $w_s(x, 0)$, the reflected surface wave is given explicitly by

$$w_s(x, 0) = \frac{D_-^*(-i\alpha)\, p_-(i\alpha)}{D_-^*(i\alpha)\, p_-(-i\alpha)}\, C_o\, e^{i(\pi - \alpha x)} \quad . \tag{30}$$

All quantities in (30) have been explicitly defined except the ratio $D_-^*(-i\alpha) / D_-^*(i\alpha)$. This ratio has one form when λ_a and λ_b are real, and different forms when λ_a and/or λ_b are imaginary. For the particular case when λ_a is real and λ_b is imaginary (that is, $-i\lambda_b$ is positive real)

$$\frac{D_-^*(-i\alpha)}{D_-^*(i\alpha)} = \exp \frac{2\alpha}{\pi} \int_o^{-i\lambda_b} \tan^{-1} \frac{4(\beta^2+\xi^2)(\lambda_a^2+\xi^2)^{1/2}(-\lambda_b^2-\xi^2)^{1/2}}{(\lambda_b^2+\beta^2+2\xi^2)^2} \frac{d\xi}{\xi^2-\alpha^2}$$

$$- \frac{2i\alpha}{\pi} \int_o^{\lambda_a} \tan^{-1} \frac{4(\beta^2-\xi^2)(\lambda_a^2-\xi^2)^{1/2}(\xi^2-\lambda_b^2)^{1/2}}{(\lambda_b^2+\beta^2-2\xi^2)^2} \frac{d\xi}{\xi^2+\alpha^2} \quad . \tag{31}$$

When λ_b is real, the first integral is absent and the lower limit of integration of the second is λ_b. When λ_a is imaginary, the lower limit of the first integral is $-i\lambda_a$ and the second integral is absent.

The ratio of the amplitude of the reflected surface wave to the amplitude of the incident surface wave versus angle of incidence

has been calculated for the special case of Poisson's ratio of 0.25, and the result is shown in Fig. 3. The wave numbers for this case are related by $\kappa_b^2 = 3\kappa_a^2$ and $\gamma^2 = 3.549\,\kappa_a^2$. Also shown in the same figure is the phase change the surface wave experiences during reflection. The values of θ_o at which β, which is the apparent wave number of the input disturbance along the reflecting barrier, equals a wave number of body waves are indicated by the lines labelled $\beta = \kappa_a$ and $\beta = \kappa_b$.

The salient features of the amplitude curve in Fig. 3 are easily interpreted. For small values of θ_o the apparent wave number β of the incident surface wave along the barrier is greater than the wave number of the slower body waves κ_b. Equivalently, the apparent wave speed of the input along the barrier is less than the shear wave speed. Consequently, only localized, non-propagating body wave modes are excited near the edge of the obstacle. All energy arriving at the obstacle in the incident surface wave must be carried away by the reflected surface wave, which is the only remaining mode of propagation. The reflection coefficient is therefore unity for $\beta > \kappa_b$. When $\beta < \kappa_b$, propagating shear waves are excited, which carry some energy away from the edge of the obstacle. The surfaces of constant phase of these shear waves are right circular cones whose axes coincide with the y-axis. The amount of energy carried by the reflected surface wave is thus reduced, as indicated by the decreasing amplitude. When $\beta < \kappa_a$, propagating dilatational modes are also excited. For reasons of symmetry, the amplitude curve has zero slope at $\theta_o = 90°$. The value of the amplitude coefficient at $\theta_o = 90°$ agrees with the result reported in [6].

Guided Surface Waves[3]

The results of the previous section are now used to obtain approximate dispersion relations for guided surface waves. The notation established in the preceding analysis will be employed here, to the extent possible. Suppose now that the motion of the surface of the elastic half-space is restricted by two rigid obstacles, leaving only a strip of finite width traction free. More precisely, suppose that the boundary conditions on $z = 0$ (5), (6), (7) are replaced by

$$\Sigma_{zz} = 0 \quad , \quad -d < x < d \quad , \tag{32}$$

$$\Sigma_{xz} = 0 \quad , \quad \Sigma_{yz} = 0 \quad , \quad -\infty < x < \infty \quad , \tag{33}$$

$$W = 0 \quad , \quad -\infty < x < -d \quad , \quad d < x < \infty \quad , \tag{34}$$

where d is the constant half-width of the traction free strip. A solution is sought for wave motion in the waveguide in the form

$$W(x, y, t) = A(x)\, e^{i(\omega t - \xi y)} \quad , \tag{35}$$

where $A(x)$ is the mode shape, ω is the frequency, and ξ is the wavenumber of the guided wave. The phase slowness of the guided wave is defined as $s = \omega/\xi$. As discussed previously, if only waves which are not attenuated as they propagate are considered, then $\kappa_b \leq \xi \leq \gamma$.

It appears to be improbable that a solution of the form (35), which satisfies the boundary conditions (32) - (34), can be found. Additional assumptions must be made, therefore, in order to obtain approximate results for the problem. To this end, it is assumed that the body

[3]The method employed in this section to construct dispersion relations evolved from several helpful discussions with Professor R. J. Clifton, Brown University.

wave disturbance localized in the vicinity of either edge of the waveguide has negligible effect on the state of deformation at the other edge. This is, in effect, an assumption on the rate at which the amplitude of the localized modes decays with distance from the edge. Although no precise information on this rate can be given, the validity of the assumption can be investigated to a limited extent. Some results are discussed in the next section. In any case, the result of the assumption is that, if a plane surface wave is incident on one edge of the waveguide, it is reflected according to the reflection law derived in the previous section. That is, the reflection from one edge of the guide occurs as though the other edge was absent. It is then possible to determine dispersion relations which are "exact" within the range of validity of the basic assumption.

The dispersion relations for a wave of the form (35) propagating in the channel are now constructed. The construction essentially consists of a superposition of wave trains which interfere in such a way as to satisfy the conditions on the edges of the waveguide. For the time being, attention is limited to those propagation modes which are symmetric, that is, $A(x) = A(-x)$. Consider two trains of harmonic surface waves propagating in the channel with angles of incidence θ_o and $-\theta_o$ and with common frequency ω. Further, suppose the two wave trains have the same amplitude, say 1/2, and are such that their crests intersect on $x = 0$. A diagram showing several lines of constant phase of these waves is shown in Fig. 4a. For definiteness, the solid lines are taken to represent crests. In the preceding section it was tacitly assumed that the phase of a wave train increases in a direction opposite to the direction of propagation. The line representing zero phase may

be selected arbitrarily, and this line is identified with a particular wave crest as shown in Fig. 4a. The dashed lines in the figure represent the lines of constant phase resulting from reflection of the zero phase lines. Denoting the phase change as a function of θ_o, which is shown in Fig. 3, by $2\pi m(\theta_o)$, the dashed lines trails the zero phase lines by a distance $2\pi m/\gamma$. The wavelength of the wave trains is $2\pi/\gamma$, of course.

The dispersion relation for symmetric waves is now obtained by combining two pieces of information. The simplest case, when any cross section of the guide is cut by at most two crests, is considered here. First, the wavelength of the guided surface wave $\ell = 2\pi/\xi$ is the interval at which the net displacement due to the combined wave trains repeats itself, that is, the wavelength is the spatial period. A wavelength is indicated in Fig. 4a, where the interval is determined by the intersection of crests. The endpoints of the interval locate lines of constant phase of the guided surface wave. Second, the phase velocity of the guided surface wave $1/s = \omega/\xi$ is the apparent speed of these lines of constant phase. Referring to Fig. 4a, the phase velocity is the speed at which the point of intersection of the crests moves along the y-axis. This information is now cast into mathematical form.

Let v denote the dimensionless phase velocity, defined as the ratio of phase velocity to surface wave velocity. Then

$$v \cos \theta_o = 1 \quad . \tag{36}$$

The wavelength ℓ is determined from the geometry of Fig. 4a to be

$$\ell = \frac{2d}{\cot \theta_o} + \frac{(1 - m)\, 2\pi}{\gamma \cos \theta_o} \quad . \tag{37}$$

The result of eliminating θ_o from (37), by employing (36), is

$$\xi d = \frac{m\pi}{(v^2 - 1)^{1/2}} \tag{38}$$

where the relation $\ell = 2\pi/\xi$ has been used. In the previous section, m was determined as a function of θ_o. In view of (36), m can alternatively be expressed as a function of v. Equation (38) is then the dispersion relation for the lowest symmetric mode of guided surface wave propagation. A plot of v versus dimensionless wave number ξd is shown in Fig. 5.

Dispersion relations for the higher symmetric modes are obtained in a similar way. These modes result when a cross section of the guide may intersect more than two crests of the wave trains. The appropriate diagram for studying the second symmetric mode is shown in Fig. 4b. Carrying out the analysis for the second and higher modes, the dispersion relation for the Mth symmetric mode is

$$\xi d = \frac{(m + M - 1)\pi}{(v^2 - 1)^{1/2}} \quad , M = 1, 2, 3, \cdots \quad . \tag{39}$$

The antisymmetric modes may be analyzed in a similar manner. The phase line diagram for the lowest antisymmetric mode is shown in Fig. 4c, where the phase zero again indicates a crest and the phase π indicates a valley. The result of analysis for the Lth antisymmetric mode is

$$\xi d = \frac{(m + L - \frac{1}{2})\pi}{(v^2 - 1)^{1/2}} \quad , L = 1, 2, 3, \cdots \quad . \tag{40}$$

The dispersion relations for the lowest antisymmetric mode and the second symmetric mode are also plotted in Fig. 5.

The means of determining mode shapes $A(x)$ resulting from superposition of wave trains propagating in oblique directions is

discussed by Tiersten [1]. The easily derived results for the problem considered here are

$$A(x) = \begin{cases} \cos\left[(v^2 - 1)^{1/2}\, \xi x\right] & \text{, symmetric} \\ \sin\left[(v^2 - 1)^{1/2}\, \xi x\right] & \text{, antisymmetric} \end{cases} \quad . \tag{41}$$

Making use of the dispersion relations, (41) becomes

$$A(x) = \begin{cases} \cos\left[(m + M - 1)\,\frac{\pi x}{d}\right] , & M = 1, 2, \cdots \\ \sin\left[(m + L - \frac{1}{2})\,\frac{\pi x}{d}\right] , & L = 1, 2, \cdots \end{cases} \tag{42}$$

It is observed that the mode shapes do not predict a zero displacement in the z-direction at $x = \pm d$, which might seem to contradict (34). The reason for this apparent difference is that $A(x)$ does not take into account the non-propagating dilatational and shear wave disturbances localized near the edges of the guide. These localized disturbances contribute to the total displacement, the net displacement being the sum of contributions due to localized modes and surface waves. The displacement due to surface waves alone is not, and indeed should not be, zero at $x = \pm d$.

Finally, the dimensionless group velocity of the various modes may be calculated directly from the dispersion relations. For the Mth symmetric mode

$$\begin{aligned} v_g &= v - \ell \frac{dv}{d\ell} \\ &= v + \frac{(m + M - 1)(v^2 - 1)}{(v^2 - 1)m' - (m + M - 1)v} \end{aligned} \tag{43}$$

where $m' = dm/dv$. For the Lth antisymmetric mode, the $(M - 1)$ in (43) is replaced by $(L - \frac{1}{2})$. Some group velocity curves of v_g versus ξd are shown in Fig. 6.

Discussion

The dispersion curves shown in Fig. 5, as well as those for all higher modes, are asymptotic to $v = 1$ as $\xi d \to \infty$. That is, for wavelengths which are infinitely short compared to channel width, waves in the channel propagate at the Rayleigh wave speed. The curves are arranged in a familiar way, with the first antisymmetric mode lying between the two lowest symmetric modes. The cut-off wavenumber of each mode is determined as the wavenumber at which the phase velocity of the guided wave equals the velocity of shear waves in the half-space. For wavenumbers outside of this range free waves cannot exist. For dimensionless wavenumbers between 2.51 and 6.21 only the lowest symmetric mode can exist, for ξd between 2.51 and 9.91 only the lowest symmetric and lowest antisymmetric modes can exist, and so on.

From the group velocity curves in Fig. 6, it is observed that the short wavelength, high frequency components of a guided pulse will propagate faster than the long wavelength, low frequency components. Due to the small variation of group velocity over the whole range of wavelengths, however, the guide must be relatively very long before this feature is advantageous for cleaning high frequency noise out of a signal. Also, out of all components of a given wavelength, the contribution of the lowest mode travels slower than the higher modes.

In the previous section, dispersion relations for guided surface waves were derived under the assumption that the body wave disturbances, localized in the vicinity of each edge of the guide, had no effect on the reflection of surface waves at the opposite edge of the guide. As a result of this assumption, the dispersion relations were obtained without direct reference to the localized disturbances. The localized

modes are represented by the branch line integrals mentioned in the process of evaluating (29) for $w(x, 0)$. Because of the complicated expressions involved in these integrals, it seems unlikely that a direct evaluation as a function of distance from the reflecting boundary can be carried out. If such an evaluation could be made it would aid in establishing a minimum distance at which, for a given wavenumber, the amplitude of the decaying part is small enough to be neglected, as was done here. Some information can be obtained, however, by asymptotic methods.

For $x < 0$, the path of integration of (29) may be completed by an arc at infinity in the right half of the λ-plane. By applying Cauchy's theorem, $w(x, 0)$ is shown to consist of a surface wave contribution (30) plus the desired branch line integral. The form of this integral makes it ideally suited for application of Laplace's method to determine the asymptotic value of the integral as $|x| \to \infty$ (see [9], for example). The result of this calculation is

$$w(x, 0) \simeq K|x|^{-3/2} e^{\lambda_b x} \quad \text{as} \quad x \to -\infty \quad , \tag{44}$$

where K is a constant. The result (44) may be used as an approximation for values of x greater than five or six wavelengths. Relation (44) implies a fairly fast decay of the localized disturbance. Because of the appearance of the algebraic factor $|x|^{-3/2}$, the decay is fairly fast even when λ_b is very small. For example, when $\lambda_b = 0$, $w(-2d, 0)/w(-d, 0) \simeq 0.36$ or when $\lambda_b = 1/d$ the ratio is about 0.13.

Additional information concerning the basic assumption can be deduced from application of the appropriate Tauberian theorem of Laplace transform analysis [8]. Consider $\partial w(x, 0)/\partial x$, obtained by differentiating

(29). From the fact that the integrand is $O(\lambda^{-1/2})$ as $|\lambda| \to \infty$, it can be deduced that $\partial w/\partial x$ is $O(|x|^{-1/2})$ as $x \to 0^-$. Since $w_s(x, 0)$ has a finite slope at $x = 0$, the localized disturbance has an infinite slope there. While it is not clear from the foregoing whether $w(x, 0)$ due to the body waves increases or decreases with distance away from the edge $x = 0$, the latter is most plausible.

Finally, the magnitude of the z component of surface displacement at $x = 0$ can be found. It is that displacement which must be added to the (known) surface wave displacement so that the net displacement is zero. This magnitude usually comes out to be less than one-half the displacement due to surface waves. Thus, based on the amplitude of the localized disturbance at $x = 0$, on the infinitely large rate at which the amplitude changes near $x = 0$, and on the fairly fast decay of the amplitude for large $|x|$, the basic assumption seems to be a reasonable one.

The limited range of applicability of the Wiener-Hopf method limits the number of surface wave reflection problems which can be solved in detail. For example, the problem which is identical to that considered here, except that all components of surface displacement are required to vanish for $x > 0$, cannot be solved by the methods employed here. The reason for this is that application of Laplace transforms yields a system of Wiener-Hopf equations, rather than a single equation, and no means of solving such systems is known [5]. There are several other configurations, besides the one considered here, which do lead to solvable Wiener-Hopf equations.

References

1. Tiersten, H. F., "Elastic Surface Waves Guided by Thin Films", Journal of Applied Physics, Vol. 40, 1969, pp. 770-789.

2. Knowles, J. K., "A Note on Elastic Surface Waves", Journal of Geophysical Research, Vol. 71, 1966, pp. 5480-5481.

3. Freund, L. B. and Achenbach, J. D., "Waves in a Semi-Infinite Plate in Smooth Contact with a Harmonically Disturbed Half-Space", International Journal of Solids and Structures, Vol. 4, 1968, pp. 605-621.

4. Stern, E., "Microsound Components, Circuits, and Applications", Microwave Theory and Techniques, IEEE Trans. Vol MTT-17, 1969, pp. 835-844.

5. Noble, B., The Wiener-Hopf Technique, Pergamon, New York, 1958.

6. Fredricks, R. W. and Knopoff, L., "The Reflection of Rayleigh Waves by a High Impedance Obstacle on a Half-Space", Geophysics, Vol 25, 1960, pp. 1195-1202.

7. de Hoop, A. T., "Representation Theorems for the Displacement in an Elastic Solid and their Application to Elastodynamic Diffraction Theory", D.Sc. thesis, Technische Hogeschool, Delft, The Netherlands, 1958.

8. van der Pol, B. and Bremmer, H., Operational Calculus, Cambridge, 1964.

9. de Bruijn, N. G., Asymptotic Methods in Analysis, North-Holland, Amsterdam, 1961.

Figure Captions

Fig. 1 The physical system viewed along the negative y-axis and the positive z-axis.

Fig. 2 The complex λ-plane for the case when λ_a is real and λ_b is imaginary, including the Laplace transform inversion path.

Fig. 3 Dimensionless amplitude and phase change of z component of displacement versus angle of incidence for surface wave reflection.

Fig. 4 Diagrams used to determine dispersion relations for (a) lowest symmetric mode, (b) second symmetric mode, and (c) lowest antisymmetric mode. The phases of the various lines of constant phase are shown.

Fig. 5 Dispersion curves for first and second symmetric modes and first antisymmetric mode, showing dimensionless phase velocity versus dimensionless wavenumber.

Fig. 6 Group velocity curves for first and second symmetric modes and first antisymmetric mode, showing dimensionless group velocity versus dimensionless wavenumber.

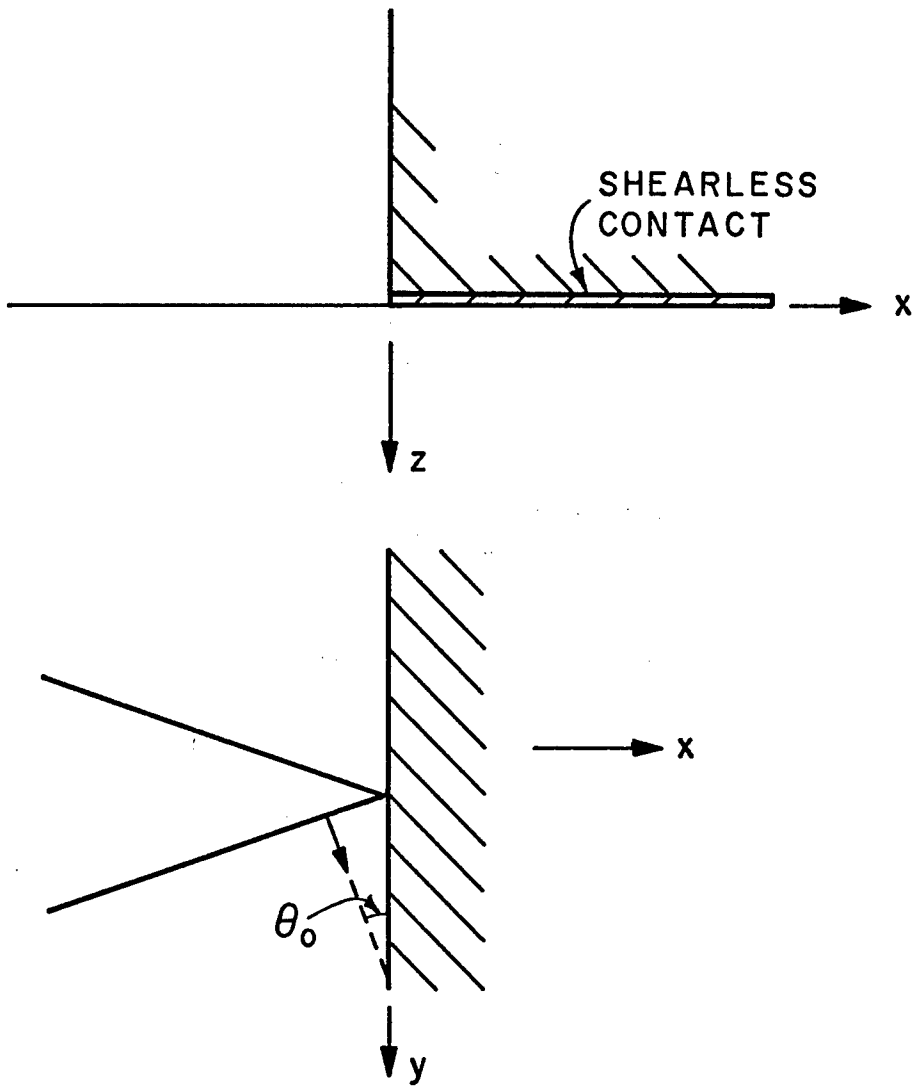

FIGURE 1

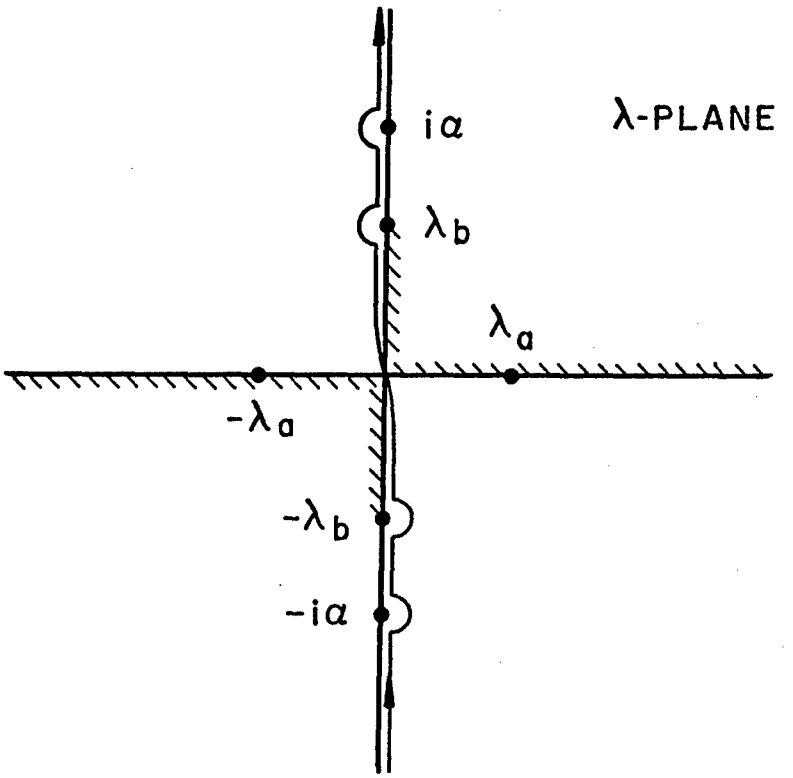

FIGURE 2

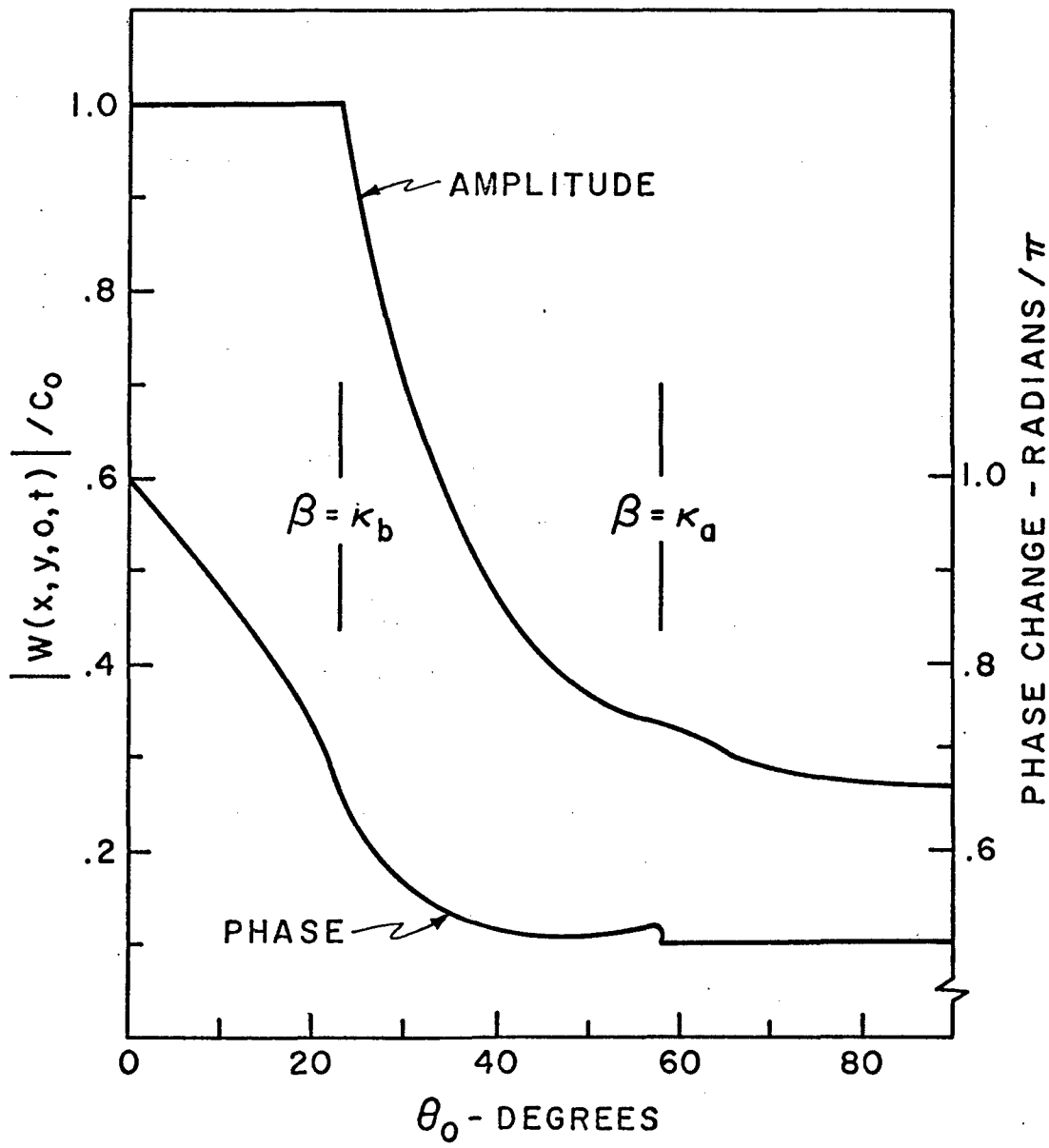
1.0
.8
.6
.4
.2
AMPLITUDE
PHASE
$\beta = \kappa_b$
$\beta = \kappa_a$
$|W(x,y,o,t)|/c_o$
1.0
.8
.6
PHASE CHANGE - RADIANS / π
0
20
40
60
80
θ_o - DEGREES

FIGURE 3

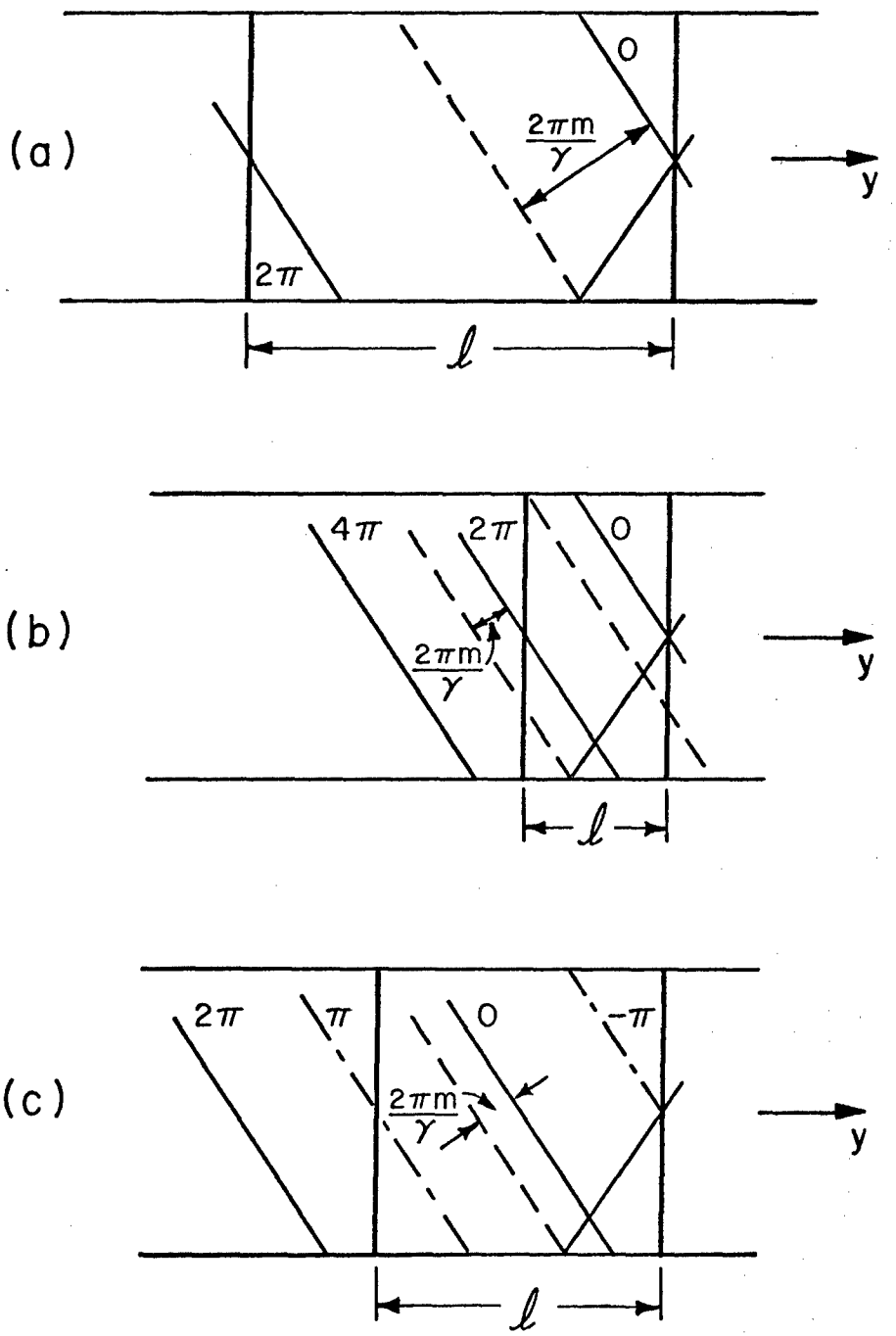

FIGURE 4

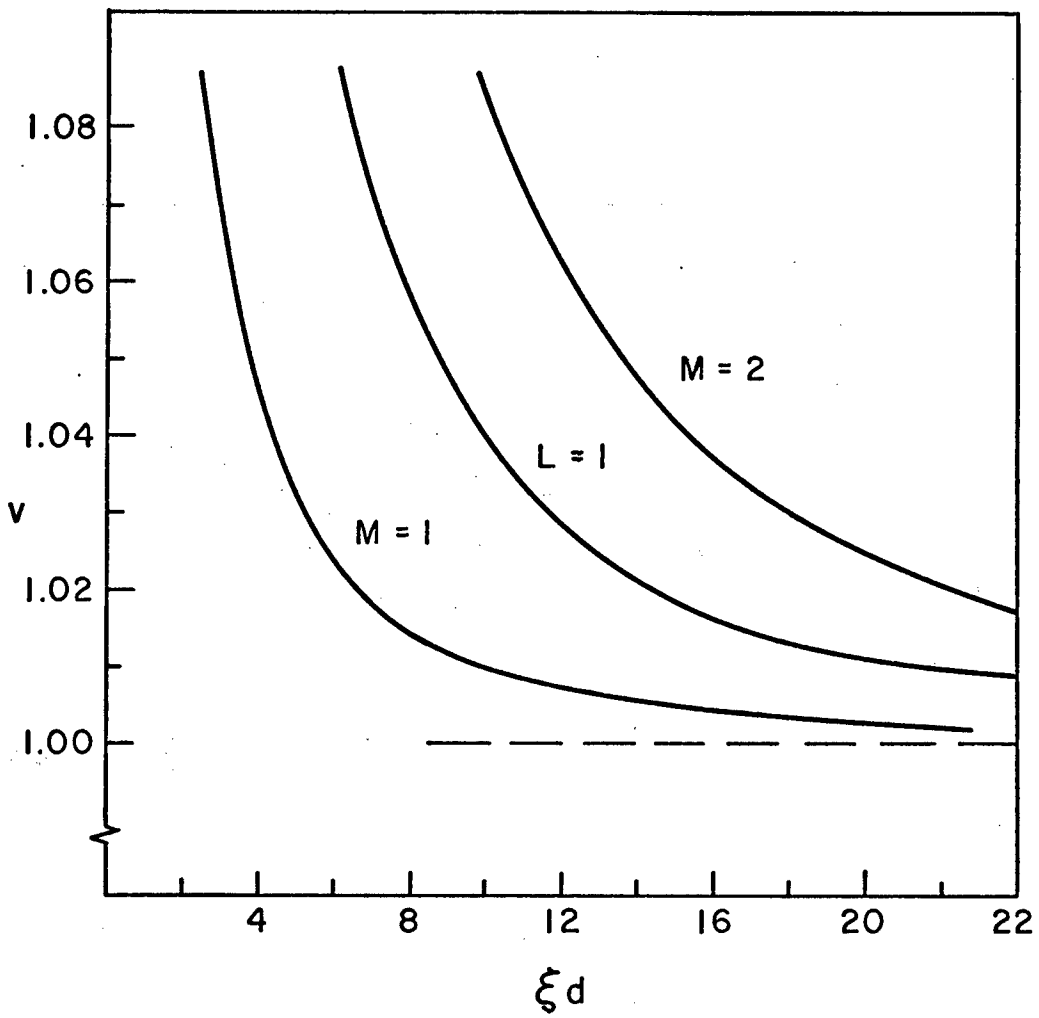

FIGURE 5

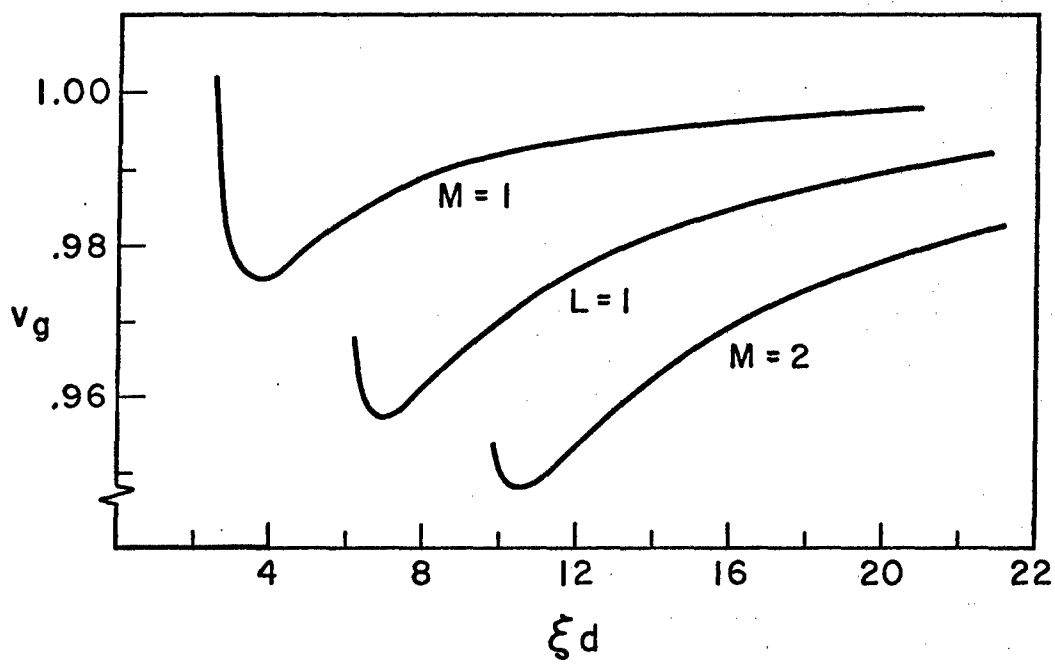

FIGURE 6